Measurement of the size distribution of multimodal colloidal systems by laser diffraction

Yiwen Pei,[1,a] Beth A. Hinchliffe,[1,a] Caterina Minelli[1]*

[1] National Physical Laboratory, Hampton Road, Teddington TW11 0LW (UK)

[a]Y.P. and B.A.H. contributed equally to this work as first authors

* caterina.minelli@npl.co.uk

ABSTRACT (250 words)

Laser diffraction (LD) is a well-established tool for the measurement of particle size distribution. Recently, its demand and use for the measurement of complex biological system have increased. Among the challenges that these types of samples present, there is the presence of multiple particle populations whose modal size may span across several orders of magnitude. In this study we assessed the accuracy of laser diffraction for the measurement of the modal diameter of both single and mixed populations of polystyrene particles with diameters ranging from 60 nm to 40 µm. We discuss the application of different available algorithms to the analysis of the data and their impact on the measurement results. Independent methods were applied to guide the selection of the algorithms and validate the measured size distributions. We found that the modal diameter of the particle size distribution measured by LD for the mixed suspension was accurate within 2 % for particles larger than 1 µm and generally within 25 % for the particles tested. Method repeatability was found to be robust, with deviations below 1 %. The method was also found to be useful for estimating the relative concentration of the particle populations in the mixed samples. This study provides confidence in the use of laser diffraction for the measurement of complex multimodal colloidal samples.

INTRODUCTION

From biomanufacturing industrial processes,[1, 2] to the development of advanced therapeutics[3-5] and encompassing ecosystem surveys,[6-8] there is an increasing need for analytical tools capable of rapidly measuring critical quality attributes of complex biological particle samples. The analysis of these particles, for example in terms of their size distribution, presents a range of challenges, including the presence of multiple populations such as protein agglomerates[9] and different types of cells spanning a broad size range from the sub-micrometre level to several tens of micrometres.[10, 11] Other challenges[12-15] include: refractive indexes similar to that of the surrounding medium, which makes the particles weakly scattering; the broad size distribution of single populations; the dynamic nature of the systems; a complex surrounding media (background); and the non-rigid and non-spherical shapes that may be encountered.

Laser diffraction (LD) is an ensemble method for rapidly measuring the size and size distribution of powder particles and colloidal systems, typically from 0.1 µm to a few millimetres in size.[16] It is widely applied in the food,[17-21] agriculture,[22-25] construction[26-28] and pharmaceutical industry.[29-31] Although LD is traditionally used to measure inorganic and synthetic particle materials, in the last few decades there has been growing interest in using LD alongside microscopy and flow cytometry for measuring more complex biological systems which often contain multimodal particle populations, such as fungi,[32] spores,[33] bacteria,[34] cell clumps or pellets[35, 36] and phytoplankton.[8] LD complements microscopy in the analysis of biological samples, with the advantage of being non-destructive, requiring minimum sample preparation and producing statistically relevant size distributions significantly faster than microscopic analysis. Rønnest and co-workers[36] have conducted a comparison study to measure the size of the cell clumps and pellets of *Streptomyces coelicolor* using LD and optical microscopy. They have found that both techniques produced consistent size information, but at least 50 microscope images had to be acquired and analysed by optical microscopy to achieve statistically meaningful sampling, while LD produced similar information in a few minutes. Leuschner *et al.* have also demonstrated a good agreement between LD- and scanning transmission electron microscopy (STEM)-determined particle sizes of *Bacillus* spore suspensions. They found that, equipped with optical microscopy, LD can be used to distinguish between spores, vegetative cells and other particles in a suspension, which is of great interest to the separation industry[33]. In another study, Leroux and co-workers showed that while cytometry and microscopy allowed for the

identification of biological particles comprised in marine samples, laser diffraction delivered in-situ, rapid, depth-resolved size distributions of particle populations with high resolution[8].

The measurement of multimodal samples is particularly challenging and most rapid ensemble methods do not perform well as they typically model the particle samples as perfect spheres with uniform size.[37, 38] Microscopy methods are suited to the analysis of complex multimodal samples, but for such samples they are time consuming and prone to artefacts and bias in sampling resulting from the sample preparation. Furthermore, vacuum methods such as electron microscopy are poorly suited for biological samples. Innovations such as cryo-transmission microscopy are step-change technologies for the microscopy of biological samples but require highly skilled operators and suffer from high costs, long measurement and analysis times and complex sample preparation. Several extensive publications[39-45] detail particle size distribution measurement by LD for polydisperse samples. However, only a few studies[46, 47] looked at multimodal colloidal systems consisting of both large and submicron particles. With recent innovations nano- and bio-technology, there is increasing demand for using LD to measure industrial samples that are heterogenous in size range and structure, where separation into constituents for analysis is not a straightforward option. In addition to measuring size and size distribution, LD offers the potential to estimate relative particle concentration,[35] although this is a broadly unexplored capability.

Herein, we evaluate the accuracy and precision of LD measurements of size, size distribution and relative concentration of ideal monomodal and multimodal polystyrene particle samples. The particle sizes, here from ~60 nm to ~40 µm, were chosen for their relevance to typical biological particles such as cells, bacteria, platelets and protein aggregates. We validate the data measured by LD by comparison to independent methods, including, dynamic light scattering (DLS), differential centrifugal sedimentation (DCS) and scanning electron microscopy (SEM). We believe this study will increase the user awareness of the LD method and improve best practice for the preparation and analysis of complex samples in many industrial sectors, from biomanufacturing, to therapeutics, to marine ecology.

METHODS

Materials: Polystyrene particle with diameter ranging between 60 nm and 40 µm were either purchased from ThermoFisher Scientific (ThermoFisher Scientific, Massachusetts, USA) as NIST traceable size standards or synthesized in house following procedures described elsewhere.[48] Details of each of the particles are summarised in Table 1. Multimodal samples were prepared by mixing equal masses (1:1:1:1:1) of five particle sets, namely PS125, PS400, PSM2, PSM21, and PSM40. The volume of solution for each sample was calculated based on their nominal mass concentration and measured gravimetrically before mixing. All samples were further diluted gravimetrically in ultrapure water.

Table 1. Sample reference and nominal mean diameter.

Sample Name	Mean Diameter[a] (µm)
PS60	0.060 ± 0.004
PS125	0.125 ± 0.003
PS197[b]	0.197 ± 0.005
PS400	0.400 ± 0.009
PS590[b]	0.591 ± 0.008
PSM2	2.0 ± 0.1
PSM21	21.0 ± 0.8
PSM40	39.6 ± 1.5

[a]Manufacturer-reported mean diameters from Coulter multisizer, transmission electron microscopy (TEM) or dynamic light scattering (DLS).
[b]Polystyrene particles synthesized in house following procedure describe elsewhere[49].

For the electron microscopy investigation, samples were prepared on Si/SiO_2 substrates. Before deposition, the substrates were cleaned by sonicating them in isopropanol for 20 minutes, then pure water for 20 minutes and finally isopropanol for a further 5 minutes. The surface was dried with compressed air and made hydrophilic by applying UV/ozone plasma cleaning for 25 minutes. 10 µL to 20 µL of colloidal polystyrene at the

concentration of 1 wt% in ultrapure water were dropped onto the surface of a clean substrate and allowed to air dry prior to the analysis.

Laser Diffraction (LD). LD analyses the diffraction pattern generated by a particle sample when exposed to a collimated beam of light. The light intensity values and relative diffraction angles are measured and used to infer a particle size distribution according to Mie theory and by modelling the particles as perfect uniform spheres. For non-transparent particles with diameters larger more than 40 times the laser wavelength, the Fraunhofer diffraction model can also be used with no requirement of knowledge of the optical properties of the particles.[17] The size distribution measured by LD is typically called a density distribution or a frequency distribution by some instrument manufacturers.[50] This is generated by using proprietary mathematical algorithms for the conversion of the light scattering pattern into a particle size distribution. We evaluated the use of different algorithms for the analysis of the data. Where required for comparison with data generated with other methods, the frequency distributions were converted to volume distributions (see below).

LD measurements were performed with a Mastersizer 3000 equipped with the Hydro MV dispersion unit (Malvern Panalytical Ltd., UK) and software v.3.71. Two light sources were used in sequence: a Helium-Neon laser emitting red light (4 mW, wavelength of 632.8 nm) and a blue LED light source (10 mW, wavelength of 470 nm). The polystyrene particle size distribution was calculated using Mie theory and a refractive index of 1.59 and 1.60 (Malvern Instruments) for the red laser and blue LED source respectively. The refractive index of water was set at a value of 1.33 for both wavelengths. The particle concentrations and stir speed were optimised prior to the measurements. Five consecutive measurements were performed for each sample and uncertainties were determined as the standard deviation of these five replicate measurements. Full details of the measurement parameters can be found in Table S1 of the Supporting Information.

Differential Centrifugal Sedimentation (DCS). DCS measures the time it takes particles to sediment through a fluid in a centrifugal field. While sedimenting, the particles separate based on their size and density and a photodetector at the edge of the disk measures their extinction. According to Stokes' law, the diameter D_s of the equivalent sphere having the same sedimentation time t_s as the particle sample and density ρ_s is expressed by equation (1):

$$D_s = D_c \sqrt{\frac{(\rho_c - \rho_f)t_c}{(\rho_s - \rho_f)t_s}} \qquad (1)$$

Here, t_c is the sedimentation time of the calibrant through the gradient of average density ρ_f, while D_c and ρ_c are the nominal diameter and density of the calibrant respectively.

DCS measurements were conducted with a CPS 24,000 Disk Centrifuge running v. 11 of the software (CPS Instruments, Prairieville, LA, USA). Prior to the measurements, a density gradient was built within the centrifuge disc, according to manufacturer instructions: the disc was filled with 14.4 mL of a sucrose (Fisher Scientific, Loughborough, UK) solution with a concentration gradient varied between 20 g/kg and 80 g/kg (average density of gradient between the particle injection and detection point is 1.011 g/mL), topped with a dodecane film (0.5 mL) to prevent evaporation. The gradient was left to thermally equilibrate for 30 minutes prior to the analysis. All measurements were performed at a wavelength of 405 nm, rotational speed of 24,000 rpm and injection volume of 100 µL. Before each sample injection, the instrument was calibrated using PS particles of diameter of 520 nm ± 5 % and density of 1.05 g/cm^3 ± 3.5 % (CPS Instruments).[51] Samples were typically diluted 1000 times in ultrapure water but concentration was optimised on a sample-by-sample basis. Full details of the measurement parameters can be found Table S2 of the Supporting Information.

Dynamic Light Scattering (DLS). DLS measures the translational diffusion coefficient of particles that are subject to Brownian motion by analysing the intensity fluctuations of laser light scattered by the particles. The particle hydrodynamic size is then determined by modelling the particles as perfect solid spheres and applying the Mie and the Rayleigh scattering theories. DLS size measurements were performed on a Zetasizer Nano (Malvern Panalytical Ltd., UK) equipped with a maximum 4 mW He-Ne laser emitting at 633 nm and Zetasizer Software, v. 7.13. Samples were contained in ZEN0040 (Malvern Panalytical) low volume disposable cuvettes. Each measurement was performed at the non-invasive back-scattering angle of 173° (in the dispersant) after thermally equilibrating the sample at 25 °C for three minutes. Samples were typically diluted 1000 times in ultrapure water but concentration was optimised on a sample-by-sample basis. The viscosity of the water was set at 0.08872 mPa·s with a refractive index of 1.33. The density distributions were converted to volume-weighted

distributions using Mie theory and refractive index and absorption values of 1.59 and 0.01 respectively. Size measurements resulting from both the cumulant method analysis and the non-negatively constrained least squares analysis (general purpose mode, i.e. regulariser parameter fixed at 0.01 for all samples) of volume-weighted size distributions were reported. Uncertainties were determined as the standard deviation of at least three replicate measurements. Full details of the measurement parameters can be found in Table S3 of the Supporting Information.

Scanning Electron Microscopy (SEM). SEM imaging was conducted with a Zeiss Supra 40 Scanning Electron Microscope (Carl Zeiss Ltd., Germany) operated at 5 keV. Working distance and pixel size were optimised for each sample. All the images were analysed using ImageJ software (version 1.52a, National Institutes of Health, USA). The particles within the images were modelled as spheres having diameter equal to the average of the maximum and minimum Feret diameters as measured by the software. The diameters of a minimum of 500 particles per sample were measured and averaged. After manual setting of contrast and circularity thresholds, that allowed only individual particles to be measured, the image analysis was automated for all samples with the exception of PSM40. The electron micrographs of sample PSM40 had poor contrast so the particles were analysed individually. The pixel size varied between 0.7 μm/pixel and 1.7 μm/pixel depending on the image magnification and resolution used for each sample. This value was used to estimate the uncertainty in the measurement of the diameter of each particle. To assess the uncertainty due to the manual setting of the contrast and circularity thresholds, these were varied between reasonable extremes on a single image. This procedure was repeated 10 times and the relative standard deviation in the average measured diameter was taken to be an estimate of the relative statistical uncertainty across all the images. The final uncertainty was calculated by adding in quadrature these contributions (Table S4).

Data Analysis. The size distributions of particle population measured by each technique were converted to volume distributions in a representation with linear abscissa to enable a fair comparison across techniques[52]. In the case of SEM, the percentage volume within each size class was calculated, using the frequencies resulting from the measured number-based size distribution and by taking the bin centre to be representative of the diameter. All distributions were fitted by using OriginPro 2019b (v. 9.65.169). Size distributions from LD and DLS measurements were fitted with LogNormal distributions. The volume-weighted size plots from the SEM measurements were plotted using Gaussian distributions. The most appropriate fit function for the DCS size distributions were chosen based on the value of the coefficient of determination R^2. The modal diameter, mean and full width half maximum (FWHM) of the fitted curves were used to compare the distributions. The mathematical expressions for these can be found in Table S5 of the Supporting Information.

RESULTS AND DISCUSSION

Monomodal distributions

Figure 1a shows the particle size distributions of monomodal PS125, PS590 and PSM2 latex suspensions as measured by LD and processed by using both the proprietary “general purpose mode” (GPM) and the “verification latex mode” (VLM) fitting algorithms (Malvern Panalytical Ltd., UK). The algorithms are designed to improve the accuracy of the measurements based on known properties of the samples. However, they can significantly change the resulting particle size distribution and they need to be applied in an informed way. According to the instrument manufacturer, the GPM is appropriate for size measurements of most analytes while the VLM is specifically designed to enable the analysis of latex standards with very narrow size distribution, such as those used during verification of the optical unit performance. The VLM algorithm essentially reduces the smoothness constraint applied during the data analysis so that the software can find a narrower solution to the particle size distribution (Internal communication, Malvern Panalytical). In Figure 1a the data treated with the VLM provides relatively narrow size distributions. In contrast, the GPM-fitted LD distributions are significantly broader for submicron samples PS125 and PS197, with lower modal diameters. For sample PSM2, however, the two algorithms provide consistent results, suggesting the choice of algorithm is less important for particles larger than a micrometre. PS125, PS590 and PSM2 were also measured by DCS and the modal diameters are reported in Figure 1a as vertical lines. Comparing the results, the VLM algorithm results in modal diameters which are consistent within 8 % or less with the DCS modal values. In contrast, the GPM algorithm significantly underestimated the diameter of the particles in samples PS125 and PS590. For sample PSM2 both algorithms provided results which were consistent with DCS measurements.

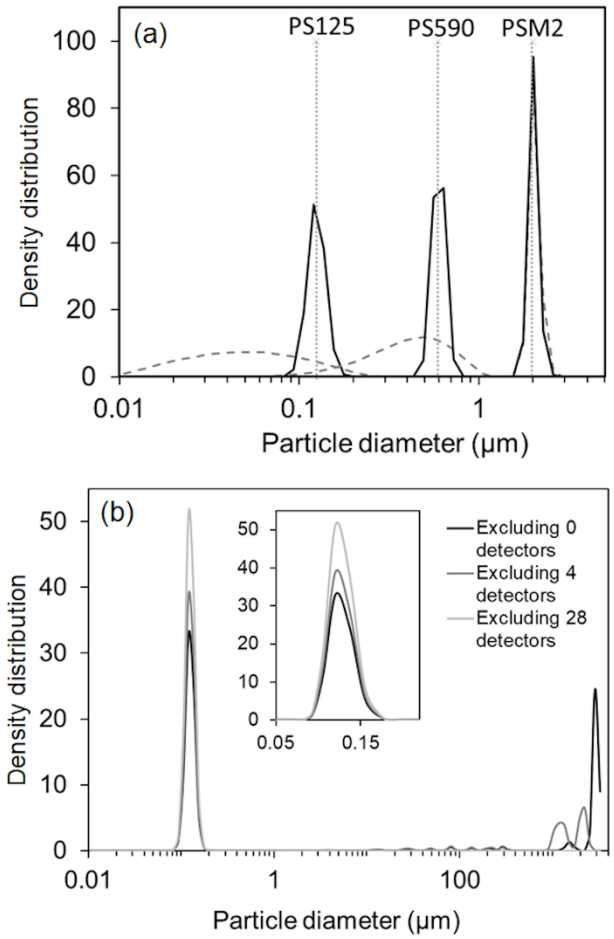

Figure 1. (a) Particle size distributions of monomodal PS125, PS590 and PSM2 as measured by LD and analysed using the VLM (solid line) and GPM (dashed line) algorithms. The dotted lines represent the reference modal diameter as measured by DCS; (b) Particle size distributions of PS125 as measured by LD and analysed with the VLM algorithm and excluding 0 (black line), 4 (grey line) and 28 (light grey line) of the detectors at low scattering angles.

Figure 1b shows that the PS125 size distribution analysed with the VLM algorithm exhibits some peaks at large diameters. These peaks may be an artefact of the measurement or indicate the presence of particles deriving from agglomeration or contamination in the sample. Potential measurement artefacts may arise when utilising the VLM algorithm as the noise at low scattering angles may be interpreted as the presence of larger particle populations and this may be enhanced by the algorithm.[53] When using the GMP algorithm some peaks at large size are still observed, but to a much lesser extent than when employing the VLM algorithm. Using the instrument software, we disabled up to 50 of the low scatter-angle detectors and observed the effect of this operation on the measured size distribution. Figure 1b shows some representative distributions to illustrate the effect of this operation: disabling the detectors led to the expected effect of removing the peaks at large diameters, accompanied with a change in the D_{50}, from 0.137 µm with 0 detectors removed to 0.124 µm with 28 inner detectors removed. No further change was observed in D_{10}, D_{50} or D_{90} when more than 28 detectors were switched off. This last value appears to be more consistent with the nominal diameter of the particles, as well as the DCS measurements. For some of the samples assessed in this work, e.g. PSM40, we took the decision to remove some of the inner detectors during the analysis. This decision was informed by knowledge from other methods. Overall, the way the data is treated during the analysis can have significant impact on the measurement results. For this reason, when the nature of the sample is not fully known, it is good practice to validate the results by measuring the size distribution of the particle samples with independent methods.

We extended the comparison of the size distributions measured by LD and independent methods to a wider size range of samples, from ~60 nm to ~40 µm, and techniques, with results shown in Figure 2 and Table 2. Here, the instrument repeatability is defined as the standard deviation between multiple measurements of the same

sample in quick succession.[17] The accuracy is defined with respect to a reference technique specified in the text. The FWHM is used to discuss resolution.[54] For particles with diameters below 10 µm, the size distribution measurements performed by LD were compared to two nanoparticle sizing techniques, DLS and DCS respectively. For particles above 10 µm, SEM was used as an independent method. These methods may apply different weighing to the size distributions they measured. To enable the comparison of the results, all measured size distributions were converted to volume-weighted size distributions.

In comparing the results between different methods, it is important to consider that each of them measures a different type of particle size depending on the underpinning physical principles. This means that the size distributions measured by different methods are not expected to be identical. Besides, the resolution of the methods also depends on the underpinning physical principle and this is reflected in the measured widths of the size distributions. DLS measures the intensity of the light scattered by an ensemble of particles in liquid and the measured diameter is the average hydrodynamic diameter. This comprises the core of the particles and any potential surface-bond molecule, including solvent molecules within the particle slipping plain. DCS measures particle light extinction as a function of sedimentation time to derive the particles' Stokes diameter, which in the case of a sphere is equivalent to the hydrodynamic diameter. Although for monodisperse spherical samples it is expected that DLS and DCS provides similar results, we should note that inaccuracies may still be introduced depending on the type of models and analysis that is applied to the data, as already discussed. SEM, on the contrary, measures a particle diameter which is closer to the physical dimension of the polystyrene core in the solid state under vacuum. LD measures the intensity of the light diffracted by the particle material and, as such, the resulting diameter is also representative of the physical polystyrene core in liquid. LD modal values are thus expected to be in general agreement with SEM and possibly lower in value with respect to DCS and DLS. It is worth noting that the number of particles tested in LD analysis can be different (typically higher) from the other methods, leading to potential differences in data statistics. Significantly, the number of particles measured by LD is several orders of magnitude higher than imaging methods. The environment experienced by the sample during measurement is also different, with potential for resulting sampling bias. During LD measurements, the sample is vortexed, also ensuring that larger particles remain suspended, which does not happen in the case of the other liquid analysis methods. For SEM measurements the sample is deposited onto substrates, placed in vacuum and probed with an electron beam, all of which may affect the structure and agglomeration of the particles.

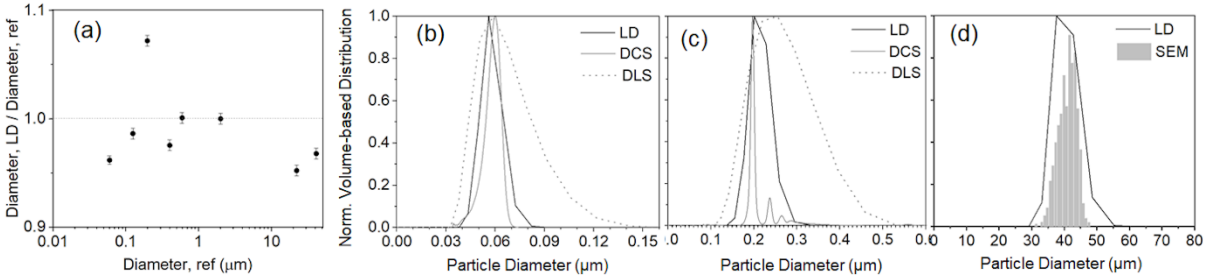

Figure 2. Validation of LD size measurements (VLM algorithm) by independent methods. (a) Ratio of diameters as measured by LD and the reference (ref) method as a function of particle size; error bars are included and represent the precision of LD. Representative size distributions are shown for (b) PS60, (c) PS197 and (d) PSM40. Graphs for the full range of particles can be found in Figure S4 in the Supporting Information.

Figure 2a shows the results of the method comparison across the size range investigated. The accuracy of the method is expressed by the distance of the data points from the dotted horizonal line, which represents the identity of the modal values measured by LD and the selected reference method. The error bars of the data points express the repeatability of the LD measurement, although they are not visible. Remarkably, the modal diameters of the volume-weighted distributions measured by LD are within 5 % of those measured by DCS and SEM except for the PS197 sample, that is discussed below. In terms of measurement precision, LD had the highest measurement repeatability among the ensemble techniques. The repeatability over 5 repeat measurements was consistently below 1 %, which is within the consensus threshold value for good measurement acceptance according to ISO 13320:2009. As far as the widths of the distributions are concerned, it is expected that both DCS and SEM measure particle size distributions with high resolution.[55] For these two techniques the ratio of the FWHM to the modal value of the distributions is consistently below 0.2, with ratios

as low as 0.04 for some distributions. DLS exhibits broader distributions with ratios between 0.5 and 0.7. For LD, the ratios range between 0.2 and 0.3, indicating that this method appears to have size resolution close to that of DCS and SEM.

Table 2. The modal diameters and FWHM values of the volume-weighted size distributions of the samples in Table 1 and the mixed sample (mix) as measured by LD, DLS, DCS and SEM. The uncertainty is the standard deviation from repeat measurements, except for SEM measurements. See the Materials section and Supporting Information for a detailed description of the fitting for all the techniques and an estimation of SEM uncertainties (Figures S1 to S4 and Table S4).

Sample	LD		LD (mix)		DCS		DLS		SEM	
	Mode (nm)	FWHM (nm)	Mode (nm)	FWHM (nm)	Mode (nm)	FWHM (nm)	Mode (nm)	FWHM (nm)	Mode[a] (nm)	FWHM (nm)
PS60	57.5 ± 0.3	15.3 ± 0.1	-	-	60 ± 2	10 ± 1	63 ± 2	36.6 ± 0.6	-	-
PS125	123 ± 1	32.8 ± 0.2	93.9 ± 0.5	24.9 ± 0.1	125 ± 2	11 ± 0.4	144 ± 2	86 ± 1	-	-
PS197	211 ± 1	56.5 ± 0.3	-	-	197 ± 4	9 ± 0.6	238 ± 4	153 ± 10	-	-
PS400	390 ± 2	67 ± 2	419 ± 2	120 ± 1	400 ± 8	27 ± 2	451 ± 4	241 ± 3	-	-
PS590	592 ± 3	116 ± 1	-	-	591 ± 10	24 ± 2	700 ± 30	340 ± 40	-	-
PSM2	2000 ± 10	295 ± 1	2010 ± 10	398 ± 2	2000 ± 40	160 ± 20	-	-	2040 ± 50	80.7 ± 0.4
PSM20	21100 ± 100	4340 ± 20	21300 ± 100	4230 ± 20	-	-	-	-	22200 ± 1700	3360 ± 17
PSM40	40000 ± 200	8400 ± 40	40700 ± 200	8970 ± 120	-	-	-	-	41000 ± 3000	7070 ± 40

Figure 2b compares the volume-based size distributions of monodisperse 60 nm particles measured by LD, DCS and DLS, with modal values and widths of the distributions recorded in Table 1. The methods are in excellent agreement. As commented before, LD measures a smaller diameter with respect to the other methods and exhibits the best measurement repeatability. The width of the distribution provides an insight into the resolution of the method. While DLS has lower resolution, LD has resolution, for these monodisperse particles, close to that of DCS, which is regarded as a high-resolution method.[56, 57]Figure 2c shows the case of an agglomerated sample, i.e. PS197. DCS is the only method with sufficient size resolution to resolve the agglomeration patterns.[48] Consequently, the peak at lower sizes in the DCS distribution is still representative of the population of non-agglomerated particles. In the case of LD and DLS, the measured distributions are monomodal and agglomeration is thus expected to impact on the method accuracy. Both DLS and LD distributions are skewed towards larger sizes, but LD to a lesser extent than DLS, with modal value 7 % larger than that measured by DCS. All the methods model the particles as perfect rigid spheres and the measured diameter is that of the "equivalent sphere" having the same physical properties measured by the instruments. The notion of equivalent sphere is particularly important for those methods that cannot resolve particle agglomeration. Both LD and DLS employ Mie's theory to convert scattered light intensity weighted distributions to volume-weighted distributions. However, while LD light intensity measurements are performed at multiple angles, DLS measurements are performed at a single angle (backscatter angle) and correlation spectroscopy is applied with a number of assumptions. The two methods have different resolutions and result in different biases in the size distribution introduced by particle agglomeration.

As previously stated, LD modal values are expected to be in general agreement with SEM. For sample PSM21, the modal values of the distributions measured by LD are 5 % smaller than the modal values measured by SEM, which is similar to the agreement that was observed for samples PSM20 and PSM40. We note that LD systematically measures a smaller diameter with respect to SEM and that the LD values are closer to the nominal diameter of the samples in Table 1, although the values are consistent when considering the associated uncertainties. It is possible that sample preparation, the electron beam, limited statistics and image analysis may all affect the accuracy of the SEM measurements, as discussed previously.

Multimodal distributions

We have discussed so far the choice of the algorithm for the analysis of the LD data and the precision and accuracy of the LD measurements with respect to the reference methods for samples made of particles with equal size. We evaluate now the ability of the LD method to resolve complex multimodal samples and the challenges that may be encountered in such measurements. As a model system, we used an equal weight mixture (1:1:1:1:1) of five monodisperse monomodal particle sets, i.e. PS125, PS400, PSM2, PSM21, and PSM40. The size range we selected for this study is significantly broad, with a size difference between the smallest and largest particle populations of greater than two orders of magnitude. This poses a significant challenge for most methods used for particle size analysis. For example, although analytical centrifugation may have the resolution to resolve the populations, the size range is a challenge and multiple measurements at different spinning velocities would be necessary to achieve similar resolutions across the populations. Electron microscopy could in principle resolve all the populations, but imaging at different resolutions would still be required to maintain the same measurement precision across them. This is in addition to the problem of the lower level of statistics already discussed. It is possible that most real-world applications do not require to address such a broad size range. Nonetheless, this sample provides us with the opportunity to discuss some issues that may be encounter when measuring polydisperse samples.

LD was capable of resolving all five populations in one single measurement when using the VLM, but not the GPM algorithm (Figure S6 of supporting information). However, the latter was still capable of identifying the correct size range of the particle populations, with the smaller populations (PS125 and PS400) merged in one broad peak with modal diameter around 200 nm, i.e. in-between the two smaller populations. The larger populations (PSM21 and PSM40) were also merged in a broad peak with modal diameter around 30 µm. i.e. also in-between the two larger populations. A third and central peak was visible with modal diameter around 2.4 µm, i.e. close to but significantly broader than PSM2.

Figure 3a shows the particle size distribution of the mixed sample, measured by LD and processed with the VLM algorithm (using all detectors), as a black continuous line. For reference, the distributions of single populations of PS125, PS400, PSM2, PSM21 and PSM40 samples are also shown with dash and dot lines. It should be noted that unlike Figure 2 density distributions are shown using a logarithmic abscissa, this is to aid the viewing of the data for the reader and the associated volume-weighted distributions on a linear abscissa can be found in Figure S7 of the Supporting Information. Remarkably, we found that the particle size distribution measured by LD for the mixed suspension was consistent with those of the monomodal samples, with deviations in the modal values below 2 % for particles larger than 1 µm. The same deviations for PS125 and PS400 were 24 % and 7.6 % respectively.

One common source of error for LD measurements that should be investigated is the use of a non-ideal particle concentration. We note that the optimal concentration depends on the optical properties of the particles and has therefore a non-monotonal dependency from their size, with the large and the small particles at the extremes of the LD sizing range requiring the largest concentrations.[53] In accordance with ISO 13320:2009, the particle concentration should be sufficiently high to produce an adequate signal-to-noise ratio but prevent multiple scattering. The latter occurs when one photon from the incident laser beam is scattered by more than one particle before reaching the detectors, that translates in an apparent shift of the distribution to lower size values. To minimise the likelihood of multiple scattering occurring, the laser obscuration measured by the instrument should fall in an appropriate range. While the concentrations of the monomodal samples could be optimised by adjusting the laser obscuration, this was not possible for each individual population of the mixed suspension as the relative concentration between the different populations is fixed. We have evaluated the impact of particle concentration on the measurement of multimodal samples. The concentration of the mixed sample used for the measurement results shown in Figure 3a represents the optimal range for the laser obscuration. Figure 3b shows the size distribution of the same mixed sample at different concentrations. As expected, different particle populations are affected differently from the selection of the sample concentration, confirming a dependency of this effect on particle size.

Sample PS125 appeared to have the opposite behaviour with respect to PS400, with the modal value measured for the mixed sample being underestimated with respect to the reference value (Figure 3a and Table1) and the peak intensity increasing with increasing concentration (Figure 3b). The reason for this behaviour is not fully understood, but could be the result of the significant complexity of the sample. PS125 is the particle population with the smallest diameter in the set and therefore lowest total scattering intensity. In comparison, as an example, PM40 has over two order of magnitude larger diameter. Although the populations scatter their

maximum intensity at different angles, the range and distributions of the scattered intensities across the angles are expected to pose some instrumental challenges.

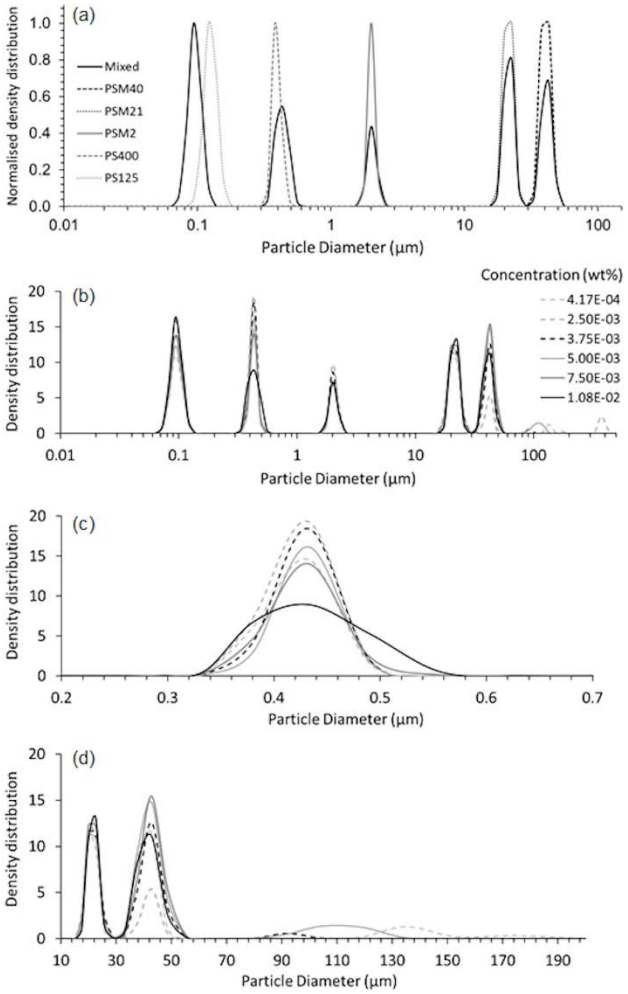

Figure 3. (a) LD particle size distributions of the individual samples PS125, PS400, PSM2, PSM21 and PSM40, as well as a mixed suspension containing equal nominal mass of all the five particle sets (1:1:1:1:1) with a total particle concentration of $9.3 \cdot 10^{-3}$ wt%; (b) Particle size distribution of the mixed suspension as measured by LD across a range of concentrations. The effect of particle concentration on the LD measured particle size distribution of (c) the PS400 population and (d) the PSM21 and PSM40 population in the mixed sample, along with satellite peaks at higher diameters; the same legend as in (b) applies. It should be noted that (a) and (b) are plotted with logarithmic scale on the X-axis, while (c) and (d) have linear scales.

Sample PS400 was one of the populations that appeared to be most affected by the particle concentration. This is shown in Figure 3c and exhibits the characteristic signs of multiple scattering, namely a shift in the distribution towards smaller diameters and a broadening of the distribution peak with increasing concentration. As a comparison, in Figure 3a the concentration of the mixed sample is $9.3 \cdot 10^{-3}$ wt% while the same value for the monomodal sample was almost 10-fold lower, at around $8.3 \cdot 10^{-4}$ wt%. This further suggests the likelihood of the occurrence of multiple scattering in the mixed sample.

Figure 3d shows that the measurement of the PSM40 population in the mixed sample is also significantly impacted by the choice of the sample concentration. At low concentrations, up to $5 \cdot 10^{-3}$ wt%, satellite peaks appear at diameters larger than 40 µm, which are most likely associated with this particle population as they appear to correlate to its variation in peak intensity. We know from the measurements performed on the single populations that these satellite peaks are likely measurement artefacts, which may occur due to the concentration of PSM40 being too low to distinguish the sample signal from the noise. As the concentration increases, these artefacts disappear and the modal value moves closer to the reference value measured by electron microscopy.

Figure 4 shows the relative changes in modal diameter, FWHM and volume with changing concentration for the mixed sample. Figure 4a shows the average modal diameter of each peak measured at different sample concentrations, relative to that measured for the single population. With the exception of PS125, the modal values measured for the particle populations in the mixed sample is within 10 % of that measured for single populations independently of sample dilution. For all samples, variability of the modal values is within 2 %, meaning that the precision of this measurement is little affected by the sample concentration. The modal value of sample PS125, however, is underestimated by 25 % with respect to the modal value measured for single populations. PS400 and PSM40 are relatively variable and the modal diameter was consistently larger than that measured for the single populations. PSM2 shows a trend of decreasing modal diameter with increasing concentration, while PSM21 shows the opposite trend.

The FWHM was less reproducible with sample concentration, with variability typically within 20%. In general, particle populations in the mixed sample exhibited larger FWHM values with respect to the measurements performed on single populations. PS125 was again an exception to the general trend. As expected from Figure 3c, the PS400 peak shows significant widening up to 50 % for concentrations above $5.7 \cdot 10^{-3}$ wt%, with the FWHM values being relatively constant at lower concentrations. As shown in Figure 4a the modal diameter was also more stable below this concentration, supporting the conclusion that both effects are the result of multiple scattering due to the increased concentration. There was also instability in the FWHM of the PSM40 peak, however this is somewhat expected given the satellite peaks appearing at lower concentrations.

The relative area under each peak relates to the relative concentration of the populations. Because the sample was created by mixing equal weights of each particle sample based on their nominal concentrations, we expect that the area of each peak in the volume-weighted size distribution is about 20 % of the total area. However PSM2 was found to have a lower concentration than the nominal value. Independent measurements by DCS revealed that, contrary to our beliefs, PSM2 had a relative mass concentration of about 30 wt% with respect to PS400. According to this result, the expected relative mass of PSM2 in the mixed sample is about 6 % of the total sample. This measured relative concentration for PSM2 is in closer agreement with LD results with respect to nominal values.

At the lowest measured concentration, all populations accounts for about 20 % of the total volume, with the exception of PSM2 which measures 10 %. Artefact satellite peaks, however, account for about 15 % of the total volume but are not included in Figure 4c. As the sample concentration increases, the areas of the satellite peaks decrease, and they are not observed for concentrations above 0.005 wt%. Above this value, all samples measure a concentration of 20 % ± 5 %, with the exception of PSM2 that measures 10 % and PS125 whose concentration increases from 26 % to 31 % with increasing concentration of total particles.

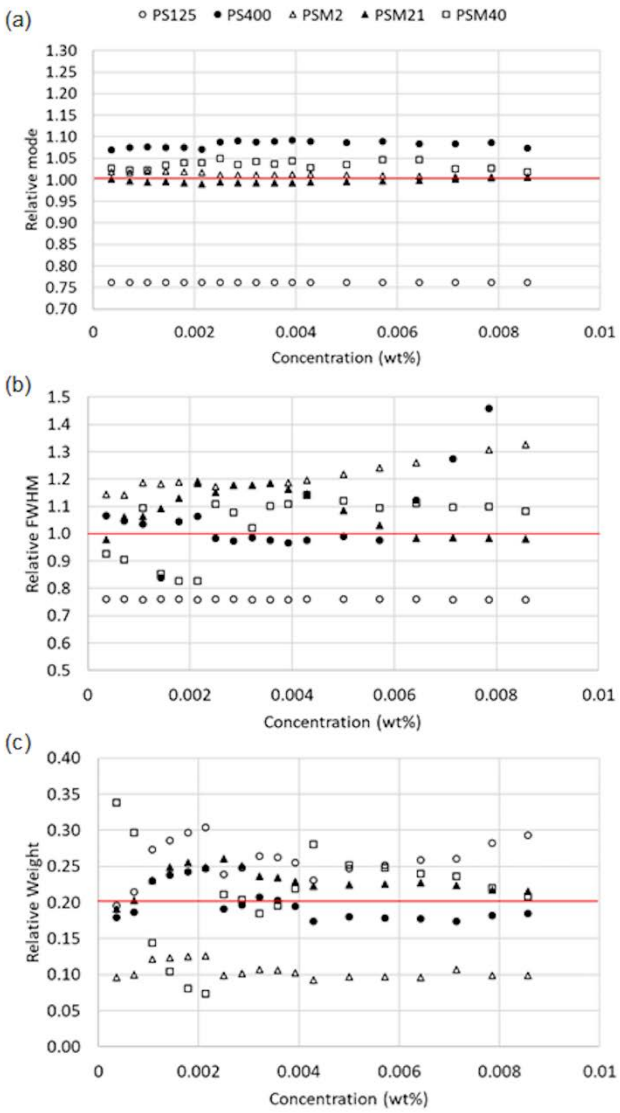

Figure 4. (a) Modal diameter of the particle population peaks in the mixed sample at the given concentration as measured from the volume-weighted size distribution, relative to the modal diameters measured for the single population. (b) FWHM of the particle population peaks in the mixed sample as measured from the volume-weighted size distribution, relative to FWHM measured for the single population. (c) Relative volume of the particle populations in the mixed sample as measured from the volume-weighted size distribution. The plot does not include the satellite peaks.

CONCLUSION

This work examined the use of LD to measure the size distribution of polystyrene beads in water comprising of both single and multiple particle populations with size ranging from 60 nm to 40 µm. In addition to the size distribution, we showed that the method is also useful for assessing the relative concentrations of the particle populations within the same sample.

For individual populations, we assessed the accuracy of the proprietary algorithm recommended by the instrument manufacturer (VLM algorithm) for the conversion of the light scattering pattern into particle size distributions by comparing the LD measurement results with independent measurement methods, namely SEM, DLS and DCS. It was noted that for unknown samples caution needs to be applied to ensure the appropriate algorithm is chosen and it is good practice that independent methods are also applied to validate the measurements results. Due to the extensive dynamic range of LD instruments, which spans from the sub-

micrometre to the millimetre scale, it was possible to resolve all the particle populations. However, it was necessary to utilise more than one independent method to cover the same size range. Furthermore, two important considerations are necessary for a meaningful comparison: (a) the particle diameters measured by different methods may be different; this is due to the different methods measuring different measurands depending on the underpinning physical principle. (b) The size distributions need to be converted to the same weighting (e.g. volume-weighted size distributions) for a fair comparison. According to our results, LD proved to be accurate within few percent for ideal samples and the most repeatable among the four sizing techniques.

For multimodal samples, LD was found to be capable of resolving the individual components of a mixture of 5 particle populations ranging from 125 nm to 40 µm when using the VLM algorithm. With the GPM algorithm, multiple populations were still identified in the correct size range, although the signal from some populations were merged to result in a broader peak with average diameter. With the VLM algorithm, when comparing the size distribution of the mixed sample with those of the monomodal samples, we found deviations in the modal values below 2 % for particles larger than 1 µm. Larger inaccuracies were found to occur for the submicron particles, which may be a result of unsuitable sample concentration and reduced scattered light intensity from the smaller particle populations with respect to larger ones. To evaluate the impact of the former on the size distributions, we performed the measurements at different sample concentration. We found that the modal values of the distributions were little affected by the concentration, with variations within 2 %. However, the width and integrals of the distributions varied up to 50 % and 70 % respectively. Remarkably, LD was also capable of providing an estimate of the relative concentrations of the particles in the mixed sample, revealing, for example, deviations of sample concentrations from nominal values.

Overall, LD was capable of delivering accurate and repeatable measurements of the size distribution of complex samples comprising particles with sizes spanning over more than two orders of magnitude. LD was also overall significantly faster than alternative high resolution methods, like, for example, electron microscopy or analytical centrifugation, which would require multiple experimental sessions with different instrumental settings to ensure similar resolution of the populations across the size range. Further advantages include that the method is non-destructive and can be implemented in/on-line. However, we note that measurement results can significantly change depending on the algorithm of choice for the data analysis and independent methods are useful to the validation of the selected analytical approach. The investigated particle size range is directly relevant for application in biology and advanced therapies and we hope this work can inform further research in these areas.

ACKNOWLEDGEMENTS

The authors thank Jason Corbett and colleagues at Malvern Panalytical for sharing useful information and stimulating discussion. We also thank Alex G. Shard for carefully reading the manuscript. The manuscript was written through contributions of all authors. BAH and YP prepared the samples, performed the measurements and contributed to data analysis and writing of the manuscript. CM conceived the work and contributed to the data analysis and the writing of the manuscript. All authors have given approval to the final version of the manuscript. NPL acknowledge funding from the UK Department of Business, Energy and Industrial Strategy through the projects NMS/IMM19 and NMS/IMM20 of the UK National Measurement System.

ASSOCIATED CONTENT

Supporting Information.

Tables of experimental parameters for LD, DCS and DLS; estimation of the uncertainty of the modal diameter measured by SEM; mathematical expression of the functions used for fitting the size distributions and related descriptors; examples of fitting for LD, DCS, DLS and SEM size distribution data; volume-based size distributions of all monomodal samples as measured by LD, DCS, DLS and SEM; volume based size distribution of multimodal sample as measured by LD using the VLM and the GMP algorithms; conversion of the volume-based size distribution as measured by LD from logarithmic to linear X-axis.

The Supporting Information is available free of charge on the ACS Publications website at DOI:XXXX

AUTHOR INFORMATION

Corresponding Author

*Email: caterina.minelli@npl.co.uk

ORCID

Beth Hinchliffe: 0000-0001-9703-0174

Yiwen Pei: 0000-0001-6976-5560

Caterina Minelli: 0000-0002-8092-251X

Funding

NPL acknowledge funding from the UK Department of Business, Energy and Industrial Strategy through the projects NMS/IMM19 and NMS/IMM20 of the UK National Measurement System.

Notes

The authors declare no competing financial interest.

REFERENCES

Uncategorized References

1. Pais, D. A.; Carrondo, M. J.; Alves, P. M.; Teixeira, A. P., Towards real-time monitoring of therapeutic protein quality in mammalian cell processes. *Curr. Opin. Biotechnol.* **2014,** *30*, 161-7.
2. Forno, G.; Ortí, E., Quality Control and Regulatory Aspects for Continuous Biomanufacturing. *Continuous Biomanufacturing-Innovative Technologies and Methods: Innovative Technologies and Methods* **2017**, 511-532.
3. Halamoda-Kenzaoui, B.; Holzwarth, U.; Roebben, G.; Bogni, A.; Bremer-Hoffmann, S., Mapping of the available standards against the regulatory needs for nanomedicines. *Wiley Interdiscip Rev Nanomed Nanobiotechnol* **2019,** *11* (1), e1531.
4. Caputo, F.; Clogston, J.; Calzolai, L.; Rosslein, M.; Prina-Mello, A., Measuring particle size distribution of nanoparticle enabled medicinal products, the joint view of EUNCL and NCI-NCL. A step by step approach combining orthogonal measurements with increasing complexity. *J Control Release* **2019,** *299*, 31-43.
5. Gioria, S.; Caputo, F.; Urban, P.; Maguire, C. M.; Bremer-Hoffmann, S.; Prina-Mello, A.; Calzolai, L.; Mehn, D., Are existing standard methods suitable for the evaluation of nanomedicines: some case studies. *Nanomedicine* **2018,** *13* (5), 539-554.
6. Borja, A.; Elliott, M.; Andersen, J. H.; Berg, T.; Carstensen, J.; Halpern, B. S.; Heiskanen, A. S.; Korpinen, S.; Lowndes, J. S. S.; Martin, G.; Rodriguez-Ezpeleta, N., Overview of Integrative Assessment of Marine Systems: The Ecosystem Approach in Practice. *Frontiers in Marine Science* **2016,** *3*, 20.
7. Borja, A.; Ranasinghe, A.; Weisberg, S. B., Assessing ecological integrity in marine waters, using multiple indices and ecosystem components: challenges for the future. *Mar. Pollut. Bull.* **2009,** *59* (1-3), 1-4.
8. Leroux, R.; Gregori, G.; Leblanc, K.; Carlotti, F.; Thyssen, M.; Dugenne, M.; Pujo-Pay, M.; Conan, P.; Jouandet, M. P.; Bhairy, N.; Berline, L., Combining laser diffraction, flow cytometry and optical microscopy to characterize a nanophytoplankton bloom in the Northwestern Mediterranean. *Prog. Oceanogr.* **2018,** *163*, 248-259.
9. Yoneda, S.; Niederleitner, B.; Wiggenhorn, M.; Koga, H.; Totoki, S.; Krayukhina, E.; Friess, W.; Uchiyama, S., Quantitative Laser Diffraction for Quantification of Protein Aggregates:

Comparison With Resonant Mass Measurement, Nanoparticle Tracking Analysis, Flow Imaging, and Light Obscuration. *J Pharm Sci* **2019,** *108* (1), 755-762.
10. Erdbrugger, U.; Lannigan, J., Analytical challenges of extracellular vesicle detection: A comparison of different techniques. *Cytometry A* **2016,** *89* (2), 123-34.
11. Lenz, M.; Roumans, N. J.; Vink, R. G.; van Baak, M. A.; Mariman, E. C.; Arts, I. C.; de Kok, T. M.; Ertaylan, G., Estimating real cell size distribution from cross-section microscopy imaging. *Bioinformatics* **2016,** *32* (17), i396-i404.
12. Minton, A. P., Recent applications of light scattering measurement in the biological and biopharmaceutical sciences. *Anal. Biochem.* **2016,** *501*, 4-22.
13. Brown, K. A.; Butler, B. J.; Sory, D.; Nguyen, T.-T. N.; Williams, A.; Proud, W. G. In *Challenges in the characterization of failure and resilience of biological materials*, 2018; AIP Publishing LLC: p 090002.
14. Rupert, D. L. M.; Claudio, V.; Lasser, C.; Bally, M., Methods for the physical characterization and quantification of extracellular vesicles in biological samples. *Biochim. Biophys. Acta, Gen. Subj.* **2017,** *1861* (1 Pt A), 3164-3179.
15. van der Toom, E. E.; Verdone, J. E.; Gorin, M. A.; Pienta, K. J., Technical challenges in the isolation and analysis of circulating tumor cells. *Oncotarget* **2016,** *7* (38), 62754-62766.
16. BS ISO 13320:2009, Particle size analysis. Laser diffraction methods. **2009**.
17. Lyu, F.; Thomas, M.; Hendriks, W. H.; van der Poel, A. F. B., Size reduction in feed technology and methods for determining, expressing and predicting particle size: A review. *Anim. Feed Sci. Technol.* **2020,** *261*, 114347.
18. Andrade, R. D.; Skurtys, O.; Osorio, F. A., Atomizing Spray Systems for Application of Edible Coatings. *Compr. Rev. Food Sci. Food Saf.* **2012,** *11* (3), 323-337.
19. Kaur, L.; Singh, J.; Singh, H.; McCarthy, O. J., Starch-cassia gum interactions: A microstructure - Rheology study. *Food Chemistry* **2008,** *111* (1), 1-10.
20. Wackerbarth, H.; Stoll, T.; Gebken, S.; Pelters, C.; Bindrich, U., Carotenoid-protein interaction as an approach for the formulation of functional food emulsions. *Food Res Int* **2009,** *42* (9), 1254-1258.
21. Borrmann, D.; Pierucci, A. P. T. R.; Leite, S. G. F.; Leao, M. H. M. D., Microencapsulation of passion fruit (Passiflora) juice with n-octenylsuccinate-derivatised starch using spray-drying. *Food Bioprod Process* **2013,** *91* (C1), 23-27.
22. Fritz, B. K.; Hoffmann, W. C.; Bagley, W. E.; Kruger, G. R.; Czaczyk, Z.; Henry, R. S., Measuring Droplet Size of Agricultural Spray Nozzles-Measurement Distance and Airspeed Effects. *Atomization Sprays* **2014,** *24* (9), 747-760.
23. Peng, H. T.; Horton, R.; Lei, T. W.; Dai, Z. C.; Wang, X. P., A modified method for estimating fine and coarse fractal dimensions of soil particle size distributions based on laser diffraction analysis. *J Soil Sediment* **2015,** *15* (4), 937-948.
24. Abarca, M.; Guerra, P.; Arce, G.; Montecinos, M.; Escauriaza, C.; Coquery, M.; Pasten, P., Response of suspended sediment particle size distributions to changes in water chemistry at an Andean mountain stream confluence receiving arsenic rich acid drainage. *Hydrol Process* **2017,** *31* (2), 296-307.
25. Montero, E., Renyi dimensions analysis of soil particle-size distributions. *Ecol Model* **2005,** *182* (3-4), 305-315.
26. Mármol, I.; Ballester, P.; Cerro, S.; Monrós, G.; Morales, J.; Sánchez, L., Use of granite sludge wastes for the production of coloured cement-based mortars. *Cem. Concr. Compos.* **2010,** *32* (8), 617-622.
27. Erdoğan, S. T.; Nie, X.; Stutzman, P. E.; Garboczi, E. J., Micrometer-scale 3-D shape characterization of eight cements: Particle shape and cement chemistry, and the effect of particle shape on laser diffraction particle size measurement. *Cem. Concr. Res.* **2010,** *40* (5), 731-739.
28. Wang, F. Z.; Liu, Y. P.; Zhang, Y. H.; Hu, S. G., Experimental study on the stability of asphalt emulsion for CA mortar by laser diffraction technique. *Constr Build Mater* **2012,** *28* (1), 117-121.

29. Jaafar-Maalej, C.; Andrieu, V.; Elaissari, A.; Fessi, H., Assessment methods of inhaled aerosols: technical aspects and applications. *Expert Opin Drug Deliv* **2009,** *6* (9), 941-59.
30. Iacocca, R. G.; Burcham, C. L.; Hilden, L. R., Particle engineering: a strategy for establishing drug substance physical property specifications during small molecule development. *J. Pharm. Sci.* **2010,** *99* (1), 51-75.
31. Naik, S.; Chaudhuri, B., Quantifying Dry Milling in Pharmaceutical Processing: A Review on Experimental and Modeling Approaches. *J. Pharm. Sci.* **2015,** *104* (8), 2401-13.
32. Hernández, D. A. Q.; Gernaey, K.; Hassager, O.; Lantz, A. E.; Hansen, K. Influence of fungal morphology on the performance of industrial fermentation processes for enzyme production. Technical University of Denmark (DTU), 2017.
33. Leuschner, R. G. K.; Weaver, A. C.; Lillford, P. J., Rapid particle size distribution analysis of Bacillus spore suspensions. *Colloids Surf., B* **1999,** *13*, 47-57.
34. Zhao, R.; Sun, J.; Torley, P.; Wang, D.; Niu, S., Measurement of particle diameter of Lactobacillus acidophilus microcapsule by spray drying and analysis on its microstructure. *World J. Microbiol. Biotechnol.* **2008,** *24*, 1349-1354.
35. Li, M.; Zhu, W.; Gao, L., Analysis of cell concentration, volume concentration, and colony size of Microcystis via laser particle analyzer. *Environ Manage* **2014,** *53* (5), 947-58.
36. Ronnest, N. P.; Stocks, S. M.; Lantz, A. E.; Gernaey, K. V., Comparison of laser diffraction and image analysis for measurement of Streptomyces coelicolor cell clumps and pellets. *Biotechnol Lett* **2012,** *34* (8), 1465-73.
37. Anderson, W.; Kozak, D.; Coleman, V. A.; Jamting, A. K.; Trau, M., A comparative study of submicron particle sizing platforms: accuracy, precision and resolution analysis of polydisperse particle size distributions. *J Colloid Interface Sci* **2013,** *405*, 322-30.
38. Fielding, L. A.; Mykhaylyk, O. O.; Armes, S. P.; Fowler, P. W.; Mittal, V.; Fitzpatrick, S., Correcting for a density distribution: particle size analysis of core-shell nanocomposite particles using disk centrifuge photosedimentometry. *Langmuir* **2012,** *28* (5), 2536-44.
39. Hackley, V. A.; Hackley, V. A.; Gintautas, V.; Ferraris, C. F., Particle size analysis by laser diffraction spectrometry: application to cementitious powders. *NIST Interagency/Internal Report (NISTIR)* **2004**.
40. Pieri, L.; Bittelli, M.; Pisa, P. R., Laser diffraction, transmission electron microscopy and image analysis to evaluate a bimodal Gaussian model for particle size distribution in soils. *Geoderma* **2006,** *135*, 118-132.
41. Smyth, H. D.; Hickey, A. J., Multimodal particle size distributions emitted from HFA-134a solution pressurized metered-dose inhalers. *AAPS PharmSciTech* **2003,** *4* (3), E38.
42. Eshel, G.; Levy, G. J.; Mingelgrin, U.; Singer, M. J., Critical evaluation of the use of laser diffraction for particle-size distribution analysis. *Soil Sci. Soc. Am. J.* **2004,** *68*, 736-743.
43. Andrews, S.; Nover, D.; Schladow, S. G., Using laser diffraction data to obtain accurate particle size distributions: the role of particle composition. *Limnol. Oceanogr.: Methods* **2010,** *8* (10), 507-526.
44. Li, H.; Li, J. W.; Bodycomb, J.; Patience, G. S., Experimental Methods in Chemical Engineering: Particle Size Distribution by Laser Diffraction-PSD. *Can. J. Chem. Eng.* **2019,** *97* (7), 1974-1981.
45. Storti, F.; Balsamo, F., Particle size distributions by laser diffraction: sensitivity of granular matter strength to analytical operating procedures. *Solid Earth* **2010,** *1* (1), 25-48.
46. Keck, C. M.; Muller, R. H., Size analysis of submicron particles by laser diffractometry--90% of the published measurements are false. *Int. J. Pharm.* **2008,** *355* (1-2), 150-63.
47. Scherer, T. M.; Leung, S.; Owyang, L.; Shire, S. J., Issues and challenges of subvisible and submicron particulate analysis in protein solutions. *AAPS J* **2012,** *14* (2), 236-43.
48. Minelli, C.; Sikora, A.; Garcia-Diez, R.; Sparnacci, K.; Gollwitzer, C.; Krumrey, M.; Shard, A. G., Measuring the size and density of nanoparticles by centrifugal sedimentation and flotation. *Analytical Methods* **2018,** *10* (15), 1725-1732.

49. Minelli, C.; Sikora, A.; Garcia-Diez, R.; Sparnacci, K.; Gollwitzer, C.; Krumrey, M.; Shard, A. G., Measuring the size and density of nanoparticles by centrifugal sedimentation and flotation. *Anal. Methods* **2018,** *10* (15), 1725-1732.
50. Boccaccini, A. R.; Erol, M.; Stark, W. J.; Mohn, D.; Hong, Z. K.; Mano, J. F., Polymer/bioactive glass nanocomposites for biomedical applications: A review. *Compos. Sci. Technol.* **2010,** *70* (13), 1764-1776.
51. Kestens, V.; Coleman, V. A.; De Temmerman, P. J.; Minelli, C.; Woehlecke, H.; Roebben, G., Improved Metrological Traceability of Particle Size Values Measured with Line-Start Incremental Centrifugal Liquid Sedimentation. *Langmuir* **2017,** *33* (33), 8213-8224.
52. BS ISO 9276-1: Representation of results of particle size analysis. Graphical representation. **1998**.
53. Panalytical, M., Mastersizer 3000 User Manual. 2017.
54. Boccaccini, A. R.; Mano, J. F., Special issue: ICCM-17: Composites in Biomedical Applications Preface. *Compos. Sci. Technol.* **2010,** *70* (13), 1763-1763.
55. Gollwitzer, C.; Bartczak, D.; Goenaga-Infante, H.; Kestens, V.; Krumrey, M.; Minelli, C.; Palmai, M.; Ramaye, Y.; Roebben, G.; Sikora, A.; Varga, Z., A comparison of techniques for size measurement of nanoparticles in cell culture medium. *Anal. Methods* **2016,** *8* (26), 5272-5282.
56. Gollwitzer, C.; Bartczak, D.; Goenaga-Infante, H.; Kestens, V.; Krumrey, M.; Minelli, C.; Pálmai, M.; Ramaye, Y.; Roebben, G.; Sikora, A., A comparison of techniques for size measurement of nanoparticles in cell culture medium. *Anal. Methods* **2016,** *8*, 5272-5282.
57. Mehn, D.; Caputo, F.; Rösslein, M.; Calzolai, L.; Saint-Antonin, F.; Courant, T.; Wick, P.; Gilliland, D., Larger or more? Nanoparticle characterisation methods for recognition of dimers. *RSC Adv.* **2017,** *7* (44), 27747-27754.